16th World Conference on Earthquake Engineering, 16WCEE 2017

Santiago Chile, January 9th to 13th 2017

Paper N° 1476 (Abstract ID)

Registration Code: S-J1464674734

Reliable Collapse Risk Assessment through Hybrid Simulation

M.J. Hashemi[(1)], H.H. Tsang[(2)], P. Rajeev[(3)], R. Al-Mahaidi[(4)], J.L. Wilson[(5)], E.F. Gad[(6)]

[(1)] *Research Fellow, Swinburne University of Technology, Australia, e-mail address: jhashemi@swin.edu.au*
[(2)] *Senior Lecturer, Swinburne University of Technology, Australia, e-mail address: htsang@swin.edu.au*
[(3)] *Senior Lecturer, Swinburne University of Technology, Australia, e-mail address: prajeev@swin.edu.au*
[(4)] *Professor, Swinburne University of Technology, Australia, e-mail address: ralmahaidi@swin.edu.au*
[(5)] *Professor and Executive Dean, Swinburne University of Technology, Australia, e-mail address: jwilson@swin.edu.au*
[(6)] *Professor, Swinburne University of Technology, Australia, e-mail address: egad@swin.edu.au*

Abstract

Collapse risk assessment of structures requires non-linear analytical models calibrated to representative experimental results, which can ideally capture the realistic collapse behaviour of structures. These analytical models, however, are often calibrated to the results from uniaxial quasi-static cyclic or monotonic tests with constant axial load, whereas many important factors that influence the response of a collapsing structure are ignored. Hybrid simulation can be used as an improved alternative to realistically apply complex time-varying boundary effects on structural components and as a result leads to more credible estimates of the collapse probability of structures. The primary objective of this paper is to conduct a comparative study to investigate the use of quasi-static (QS) versus hybrid simulation (HS) test results for collapse risk assessment of reinforced concrete (RC) structures. For this purpose, two identical limited-ductile RC columns were tested by the respective experimental methods using a state-of-the-art Multi-Axis Substructure Testing (MAST) system capable of controlling all six-degrees-of-freedom (6-DOF) boundary conditions in mixed load and deformation modes. A comparative collapse risk assessment was then conducted that highlights the significant discrepancies in the estimates of collapse probability if QS test results are used for the calibration of modelling parameters.

Keywords: hybrid simulation, multi-axis testing, mixed-mode control, collapse risk assessment, RC structures

1. Introduction

Collapse modelling and the associated risk assessment of RC structures have mainly been attempted by researchers using incremental dynamic analysis (IDA) [1] of non-linear structural models, which can be used for developing collapse fragility curves [2-5]. The parameters of non-linear models are often estimated based on empirical equations that relate the model parameters to the hysteretic response of structures [6-8]. Haselton *et al.* [6] developed regression-based empirical equations to predict the flexural response behaviour of RC columns by calibrating the parameters of the Ibarra-Medina-Krawinkler peak-oriented hysteretic model [9] to a database of 255 rectangular column tests [10].

The experimental data used for developing the empirical equations, however, typically include only uniaxial cyclic and monotonic tests with constant axial loads, which are not sufficient for accurately predicting the non-linear response and collapse behaviour of RC elements. There are two major reasons: 1) recent research findings demonstrate that the variation in axial load combined with horizontal cyclic actions may drastically change the hysteretic characteristics of RC sections [11-13], and 2) recent shake-table collapse experiments of structures [14] have demonstrated that during earthquake shaking, a structure deforms asymmetrically with large monotonic pushes and a few small inelastic cycles prior to collapse (also defined as ratcheting behaviour [9; 15]). This causes less between-cycle (cyclic) deterioration in the strength and stiffness of structural components compared to when symmetrically cyclic protocols are employed [16; 17]. These factors may greatly influence the calibration of hysteresis parameters, specifically the plastic deformation capacity, ultimate drift and force degradation, including in-cycle (post-peak negative stiffness) and between-cycle or cyclic (reduction of strength due to the large number of cycles) degradations.

Hybrid simulation can be used as an attractive alternative to mimic collapse behaviours [18-20] and evaluate phenomena that are not represented adequately in quasi-static tests. During hybrid simulation, the physical portion of the structure is embedded into the numerical model of the full structure and sits within the finite-element code. This allows for realistic simulation of the continuous time-varying load distribution during an actual seismic event [21]. The primary objective of this paper is to conduct a comparative study to investigate the use of quasi-static (QS) versus hybrid simulation (HS) test results for collapse risk assessment of RC structures. For this purpose, two identical limited-ductile RC columns were tested by the respective experimental methods using a state-of-the-art Multi-Axis Substructure Testing (MAST) system, capable of controlling all six-degrees-of-freedom (6-DOF) boundary conditions in mixed load and deformation modes. A simplified comparative collapse risk assessment was then conducted that highlights the significant discrepancies in the estimates of collapse probability when QS test results are used for the calibration of modelling parameters.

2. Multi-Axis Substructure Testing (MAST) System

The experiments were conducted in the Smart Structures Laboratory at Swinburne University of Technology using Australia's 6-DOF hybrid simulation facility, the Multi-Axis Substructure Testing (MAST) system. Multi-directional loading on structural components has been performed previously at the George E. Brown Jr. Network for Earthquake Engineering Simulation (NEES) facilities in the U.S., including the Multi-Axial Sub-assemblage Testing Laboratory located at the University of Minnesota, Minneapolis [22], which has been used for quasi-static tests, and the Multi-Axial Full-Scale Sub-Structure Testing and Simulation facility at the University of Illinois at Urbana-Champaign [23; 24], which has been used for displacement-control hybrid simulation experiments. These systems have the capacity for large-scale testing and the ability to control multiple DOFs at the boundaries of physical specimens. Building on the same concept, the MAST system at Swinburne has been established to provide a state-of-the-art facility for mixed-mode large-scale quasi-static cyclic testing and local/geographically-distributed hybrid simulation experiments [25]. Fig. 1 shows an overview of the MAST system. The key components of the 6-DOF hybrid testing facility are:

1. Four ±1MN vertical hydraulic actuators and two pairs of ±500kN horizontal actuators in orthogonal directions. Auxiliary actuators are also available for additional loading configurations on the specimen (Fig. 2 and Table 1).
2. A 9.5 tonne steel crosshead that transfers the 6-DOF forces from the actuators to the specimen. The test area under the crosshead is approximately 3m × 3m in plan and 3.2m high.
3. A reaction system comprising an L-shaped strong-wall (5m tall × 1m thick) and a 1m thick strong-floor.
4. An advanced servo-hydraulic control system capable of imposing simultaneous 6-DOF states of deformation and load in switched and mixed mode control. In addition, the Centre of Rotation (CoR) (i.e. the fixed point around which the 6-DOF movements of the control point occurs) can be relocated and/or reoriented by assigning the desired values.
5. An advanced three-loop hybrid simulation architecture [26] including: the servo-control loop that contains the MTS FlexTest controller (inner-most loop), the predictor-corrector loop running on the xPC-Target real-time digital signal processor (middle-loop) and the integrator loop running on the xPC-Host (the outer loop).
6. Additional high-precision draw-wire absolute encoders with the resolution of 25 microns that can be directly fed back to the controller.

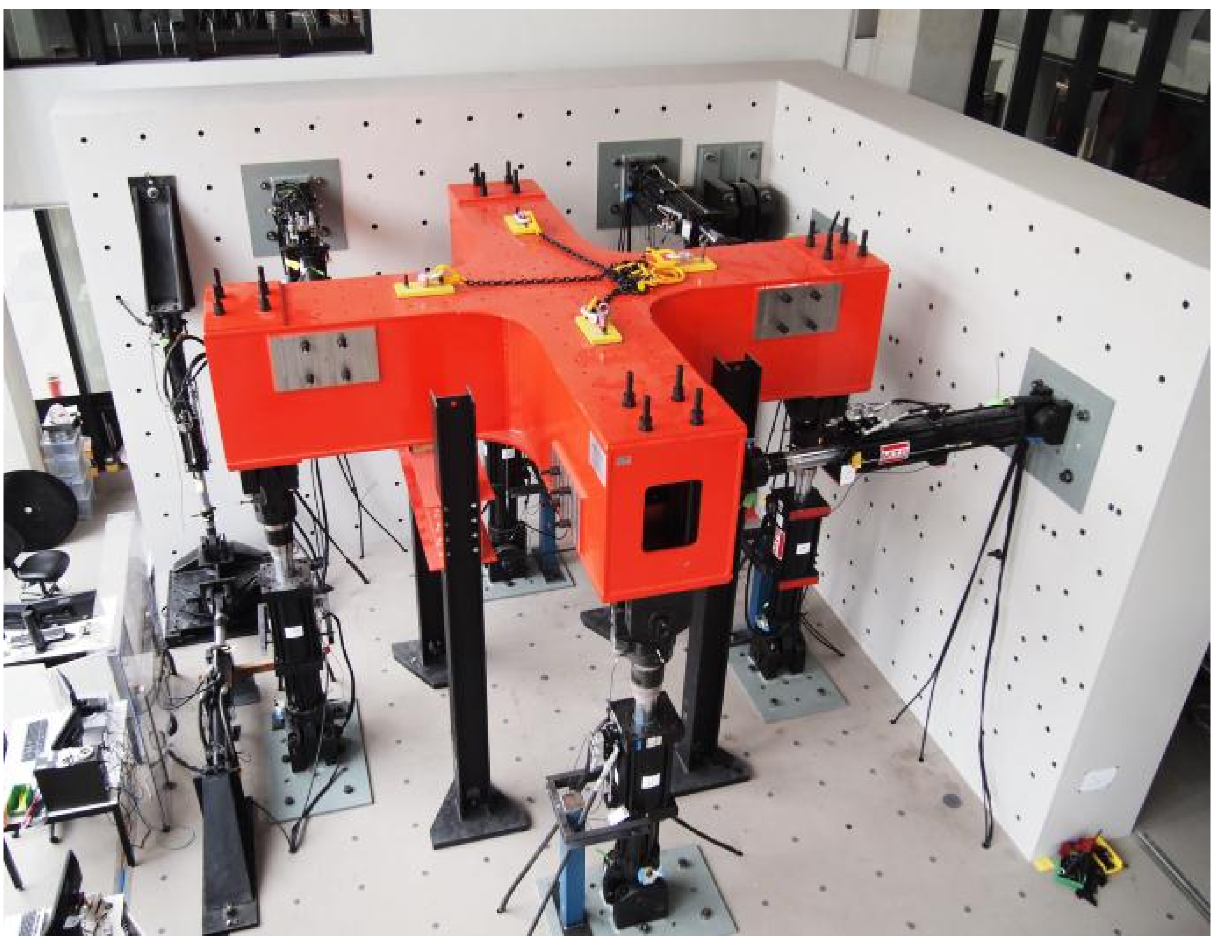

Fig. 1 – Multi-Axis Substructure Testing (MAST) system in the Smart Structures Laboratory at Swinburne University of Technology, Melbourne, Australia

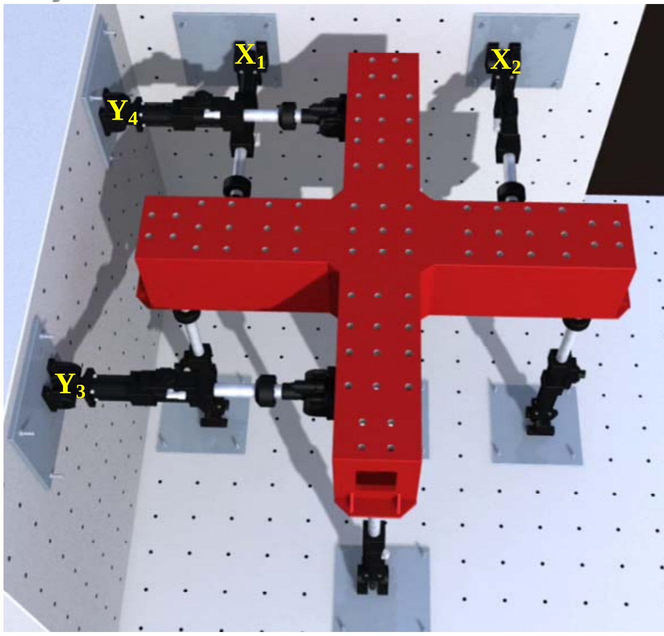

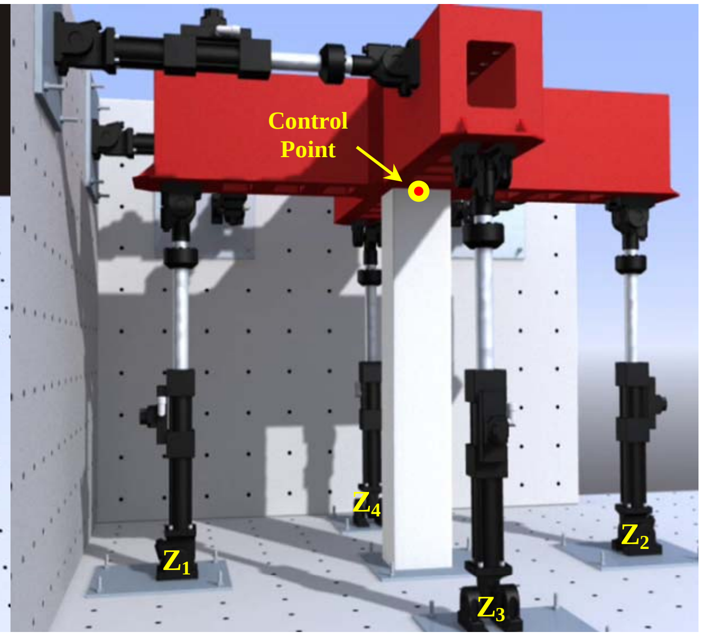

a) Actuator assembly: plan view b) Actuator assembly: side view

Fig. 2 – Actuator assemblies in the MAST system

Table 1 – MAST system specifications

MAST Actuator Capacity			
Actuator	**Vertical**	**Horizontal**	**Auxiliary**
Model	MTS 244.51	MTS 244.41	2 (MN) (Qty. 1) 250 (kN) (Qty. 4) 100 (kN) (Qty. 3) 25 (kN) (Qty. 3) 10 (kN) (Qty. 1)
Quantity	4 (Z_1, Z_2, Z_3, Z_4)	4 (X_1, X_2, Y_3, Y_4)	
Force Stall Capacity	± 1,000 (kN)	± 500 (kN)	
Static	± 250 (mm)	± 250 (mm)	
Servo-valve flow	114 (lpm)	57 (lpm)	
MAST DOFs Capacity (non-concurrent)			
DOF	**Load**	**Deformation**	**Specimen Dimension**
X (Lateral)	1 (MN)	± 250 (mm)	3.00 (m)
Y (Longitudinal)	1 (MN)	± 250 (mm)	3.00 (m)
Z (Axial/Vertical)	4 (MN)	± 250 (mm)	3.25 (m)
Rx (Bending/Roll)	4.5 (MN.m)	± 7 (degree)	
Ry (Bending/Pitch)	4.5 (MN.m)	± 7 (degree)	
Rz (Torsion/Yaw)	3.5 (MN.m)	± 7 (degree)	

3. Description of Experimental Tests

Two identical limited-ductile RC columns were tested in three-dimensional mixed-mode quasi-static (QS) and hybrid simulation (HS) experiments. The specimens were 2.5m high, had square 250mm × 250mm cross-sections and were reinforced with 4 longitudinal bars of N16 (reinforcement ratio = 1.28%) and tied with R6 stirrups spaced at 175mm with 30mm cover thickness. The specimens were attached to the strong floor from the base and to the crosshead from the top through rigid concrete pedestals.

The first experiment conducted on the RC column was a three-dimensional mixed-mode QS cyclic test. The loading protocol consisted of simultaneously applying a constant gravity load, equal to 8% of ultimate compressive load capacity in force control, while imposing bidirectional lateral deformation reversals in displacement control, following the hexagonal orbital pattern suggested in FEMA 461 [27]. The failure of the specimen occurred when the specimen was subjected to the maximum of 7.0% and 3.5% drift ratios in Y and X axes, respectively. These are large drifts for a limited-ductile column that are reasonable for the relatively low axial loads applied to the column [28] .

The second experiment conducted was a three-dimensional hybrid simulation of a half-scale symmetrical 5-storey (height of first storey h1=2.5m, height of other stories htyp=2.0m) 5×5 bay (column spacing b=4.2m) RC ordinary moment frame building. The physical specimen served as the first-storey corner-column of the building, considered as the critical element of the structure due to dynamic overturning effects and the influence of axial load variation. The rest of the structural elements, inertial and damping forces, gravity and dynamic loads and second-order effects were modelled numerically in the computer.

The structure's beams and columns were modelled using beam-with-hinges elements, where the non-linear behaviour is assumed to occur within a finite length at both ends based on the distributed-plasticity concept [29; 30]. The plasticity model follows a peak-ordinated hysteresis response based on the Modified Ibarra-Medina-Krawinkler (IMK) deterioration model of flexural behaviour [31; 32].

For the HS test, the two horizontal components of the 1979 Imperial Valley earthquake ground motions recorded at El Centro station with peak ground acceleration of 0.15g were used. Based on incremental dynamic analysis, four levels of intensity were considered to capture the full range of structural response from linear-elastic range to collapse. The selected scale factors were 0.6, 4.0, 8.0 and 9.0, which pushed the structure to nearly 0.25% (elastic), 2%, 4% and 6% inter-storey drift ratios, respectively.

Prior to conducting the actual HS test with the physical sub-assembly in the laboratory, a series of FE-coupled numerical simulations [33] was conducted to evaluate the integration scheme parameters for the actual experiments. Accordingly, generalized Alpha-OS [21] was used as the integration scheme and the integration time-step was optimized to preserve the accuracy and stability of the simulation, while allowing the completion of the entire test during the regular operational hours of the laboratory. 5% Rayleigh damping was specified to the first and third modes of vibration. Additional damping was also assigned to free vibration time intervals between the forced vibrations in order to quickly bring the structure to rest.

The hybrid simulation was started by applying the gravity load on the specimen, using a ramp function, followed by sequential ground motions. The entire sequence of loading was performed and automated using OpenSees. Considering the 117msec delay in the hydraulic system, 500msec was specified as the simulation time-step in xPC-Target predictor-corrector to provide sufficient time for integration computation, communication, actuator motions and data acquisition. This scaled the 60sec of sequential ground motions to 6 hours in laboratory time.

Fig. 3 compares the responses of RC columns including hysteresis in X and Y axes and the axial force time history in Z-axis for the QS and the HS tests. The maximum time-varying axial load applied on the specimen was 553kN in compression and 161kN in tension. Fig.4 compares the biaxial moment interactions at the top of the columns. By comparing the hysteresis plots from the HS test, it can be seen that the column was damaged as the structure progressively moved in one direction, while in the QS test the pattern of damage was symmetrical due to load reversals in cyclic deformations.

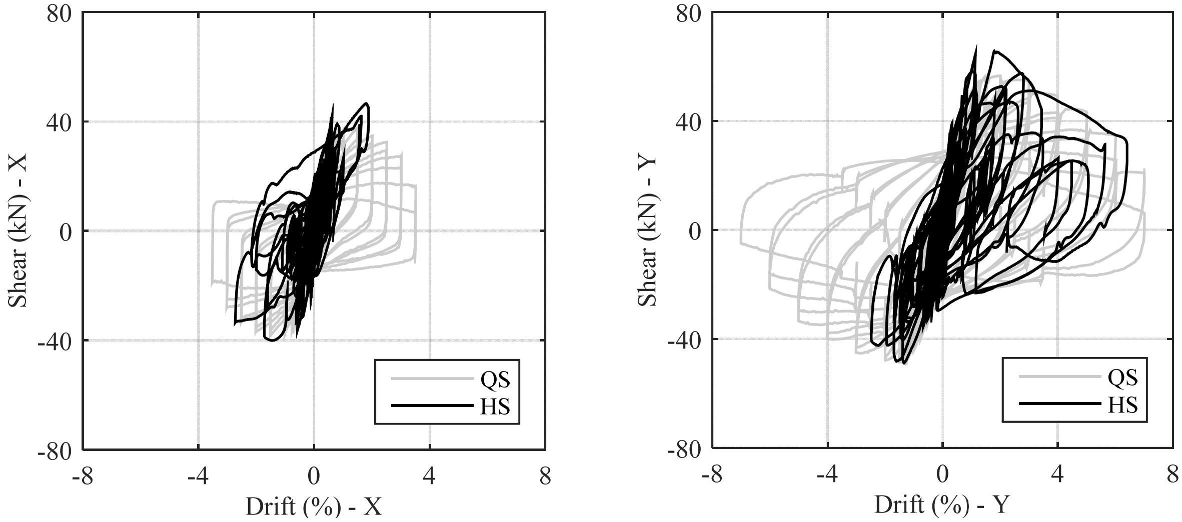

a) Comparison of the responses of RC columns in X and Y axes

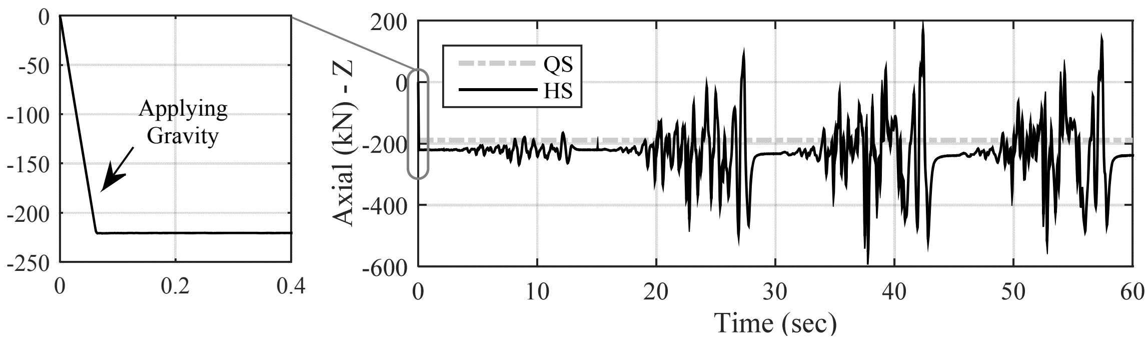

b) Axial load time history in Z axis

Fig. 3 – Response of the RC columns and applied axial load in QS and HS tests

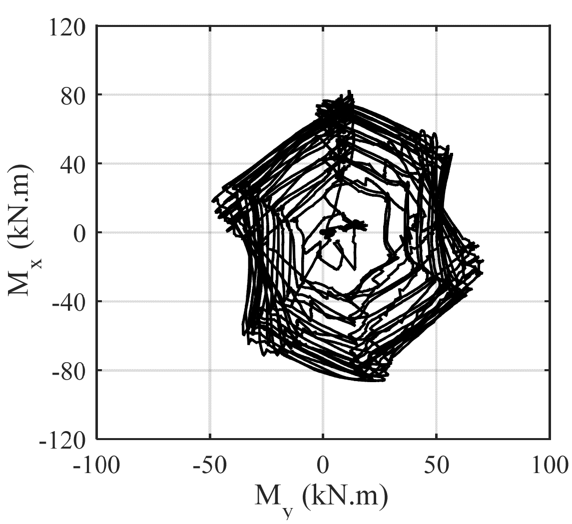

a) QS test only

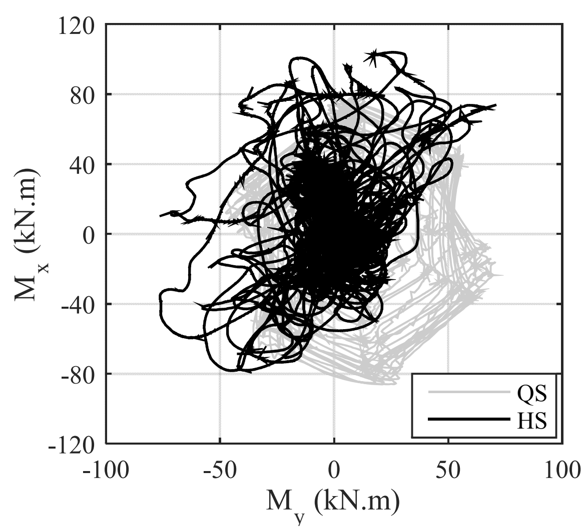

b) both QS and HS tests

Fig. 4 – Comparison of biaxial moment interactions in QS and HS tests

4. Collapse Risk Assessment

In order to investigate the influence of the selected experimental method on assessing the collapse risk of structure, a comparative collapse risk assessment for a sub-structure of the RC building was conducted using the results of the QS and HS tests respectively. As illustrated in Fig. 5, the numerical model selected for incremental dynamic analysis (IDA) includes only the first-storey corner column and the overhead mass portion of the upper 5 floors, which is equivalent to a single-degree-of-freedom (SDOF) system with a natural period of 0.6sec. This allows the study of the response of the critical element (i.e. the first-storey corner column) purely based on experimental results and removes the influence of the responses of other numerical elements.

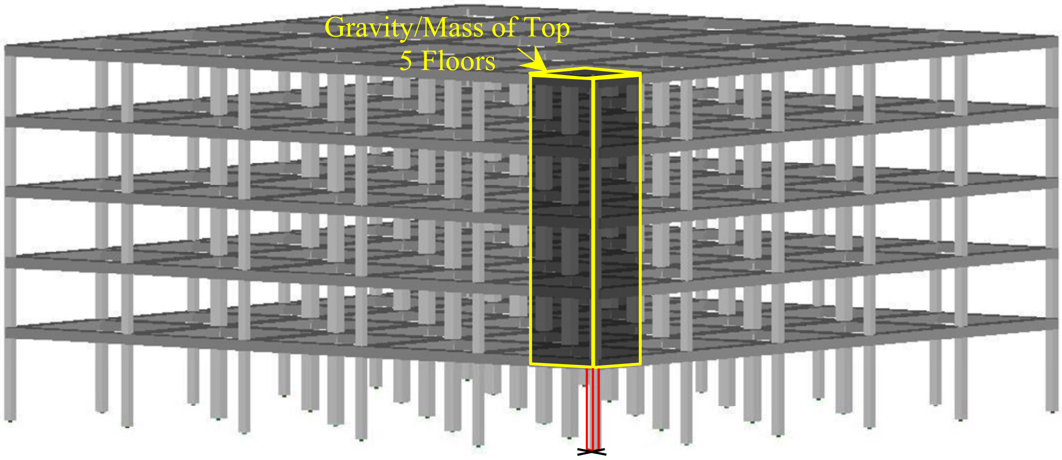

Fig. 5 – Numerical sub-structure selected for collapse risk assessment

The experimental results were used to calibrate the SDOF numerical model. The moment-curvature behaviour of the plastic zones follows the IMK hysteresis model. Although this model can generally simulate most of the important behaviours, including strength and stiffness degradation, effects such as the interaction between axial, flexure, and shear failure cannot be captured. Accordingly, a unidirectional numerical model of the column was selected and the hysteresis parameters of the IMK model were calibrated to the response of the specimen in the main axis (i.e. the Y axis of the MAST system), along which it experienced maximum deformation. Consequently, the influence of axial loads and out-of-plane moments in the experiments were implicitly taken into account by using the calibrated numerical models. Note that the use of fibre-based plasticity models may be an alternative. However, only the most basic aspects such as material constitutive relationships are modelled, while the degradation parameters that have a significant impact on collapse behaviours are not included. Fig. 6 compares the calibrated numerical model of the column to the QS and HS test results in the Y axis. Particular emphasis was placed on precisely mimicking the plastic and post-capping deformation capacities as well as the cyclic deteriorations that are known to have an important influence on collapse prediction.

IDA was performed using the calibrated numerical model in order to capture a range of probable dynamic response behaviours due to record-to-record variability in ground motion characteristics. For this purpose, three earthquake scenarios, including M6.0R28, M6.5R40 and M7.0R90 (M and R stand for magnitude and source-site distance respectively), were considered. A suite of 20 recorded ground motions was selected from the PEER database [34]. Each unidirectional ground motion was individually applied to the QS- and HS-based calibrated numerical models for the non-linear simulation. The ground motions were increasingly scaled according to the value of spectral acceleration at the natural period of the numerical model, $S_a(T = 0.6\text{sec})$, until reaching the state of collapse. The simulation was based on 5% mass-proportional damping and restricted to sidesway-only collapse with a drift limit of 7% based on the experimental results. The outcome of this assessment is a structural collapse fragility function, which is a lognormal distribution relating the structure's probability of collapse to the ground-motion intensity. Fig. 7 presents the results of non-linear IDA for the QS- and HS-based numerical models.

A lognormal cumulative distribution function was then used to define the collapse fragility functions, $P(C|z)$, which predicts the probability of collapse given a certain level of ground motion intensity, z (see Fig. 8). The computed mean and standard deviation values for QS- and HS-based numerical models show that while the dispersion of S_a is similar in both cases ($\sigma_{ln(Sa,0.6)}$ = 0.45 and 0.42 respectively), the S_a level with 50% probability of collapse is significantly over-estimated by the QS-based model (1.5g) compared to the HS-based model (1.2g).

The 2012 edition of the International Building Code (IBC) [35] and the 2010 edition of the structural design standard ASCE/SEI 7 [36] specify the performance requirement of having uniform collapse risk for structures that are designed based on the risk-targeted maximum considered earthquake (MCE_R) ground motions (with a return period around 2,500 years). Under the MCE_R ground motions, it is expected to have less than 10% probability of collapse for Risk Category I and II structures, 6% for Risk Category III structures and 3% for Risk Category IV structures. This probability, $P(C \mid MCE_R)$, of the case study structure is 1.3% and 3.9%, respectively, for the QS- and HS-based models. This indicates that a Risk Category IV structure is deemed safe if the numerical model is calibrated against QS results, but it may be considered unsafe based on HS results.

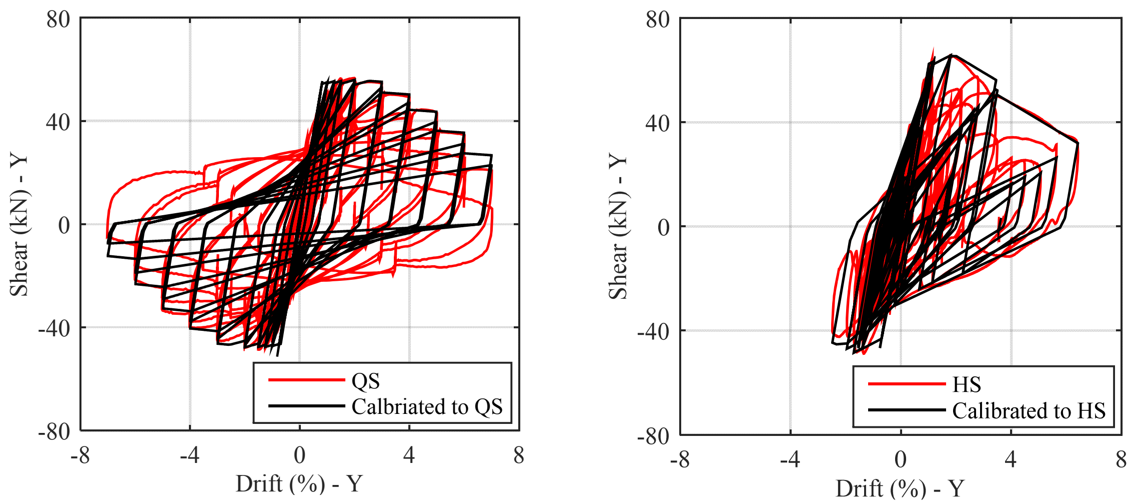

a) Calibration of SDOF model to response of RC column from QS test

b) Calibration of SDOF model to response of RC column from HS test

Fig. 6 – Calibration of SDOF numerical model to QS test results and comparison with HS test results

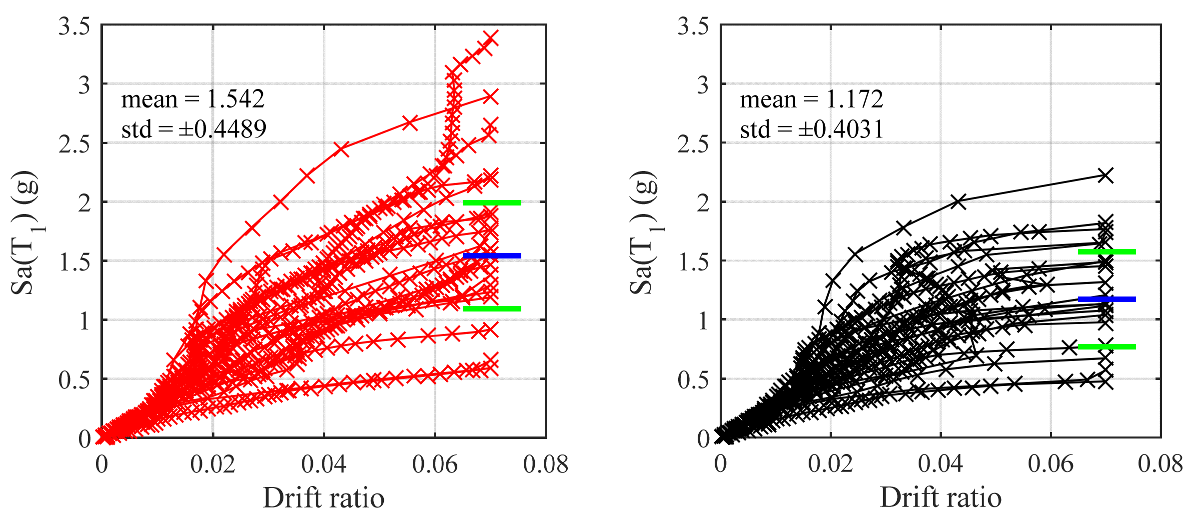

a) IDA results based on numerical model calibrated to QS test

b) IDA results based on numerical model calibrated to HS test

Fig. 7 – Comparison of IDA results for the RC column based on results from QS and HS tests

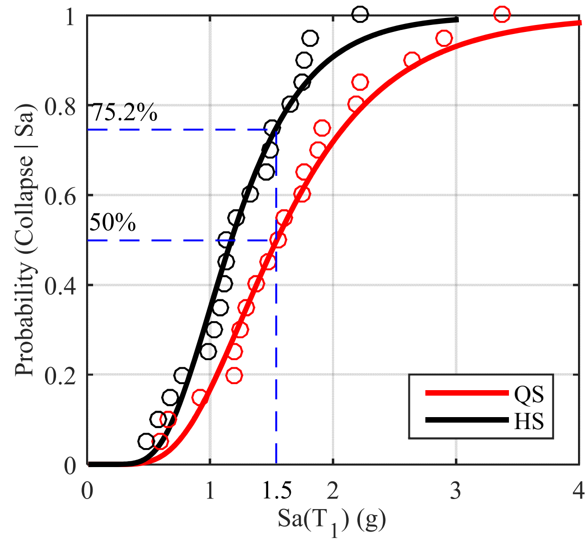

Fig. 8 – Comparison of fragility curves for the RC column based on results from QS and HS tests

IBC-2012 and ASCE/SEI 7 also specify a requirement of 1% probability of collapse in 50 years for Risk Category I and II structures, and less than 1% for Risk Category III and IV structures. The annual probability of collapse, $P(C)$, can be computed using the integral of Eq. (1):

$$P(C) = \int P(C\,|\,z) \times \left| dH(z)/dz \right| \; dz \qquad (1)$$

where, $H(z)$ is the hazard function for the ground motion parameter z, i.e. $S_a(0.6)$ in this study.

The computation of collapse probability requires seismic hazard predictions for annual frequency of exceedance as low as 10^{-5} or sometimes lower than 10^{-6}. The only set of hazard results for Melbourne, Australia that is available in the public domain can be found in Somerville et al. [37], which is therefore adopted in this study. As the natural period T of the equivalent SDOF system is 0.6sec, the corresponding hazard function in terms of $S_a(0.6)$ for rock sites can be represented by Eq. (2):

$$S_a(0.6, T_r) = 0.29(T_r\,/5000)^n \qquad (2)$$

where, T_r is the return period of the ground motion,
$n = 0.4$ when $T_r \le 5{,}000$, and $n = 0.31$ when $T_r \ge 5{,}000$.

In the present study, the upper limit of hazard is chosen as the median prediction of $S_a(0.6)$ that can be generated by an Mw 7.5 thrust faulting earthquake occurring at a close distance of 3 km on an unidentified fault (a scenario assumed in Somerville et al. [37]), which is equal to 0.92g on rock sites and has an annual frequency of exceedance of around 5×10^{-6}. A sensitivity study shows that the total collapse probability estimated for this case study building can be elevated by up to 10% if ground motions of lower frequencies of exceedance are included in the computation.

The case study building is assumed to be located on a Class C stiff soil site, with natural period of the whole soil layer, T_S, being within 0.15sec and 0.6sec, according to the refined site classification scheme [38] recommended for the Australian Standard for Earthquake Actions, AS 1170.4. It is noted that the upper boundary of 0.6sec has already been used for Class C sites in the current edition of AS 1170.4–2007 [39]. The proposed spectral amplification ratio at $T = 0.6$sec is 2.5 for Class C sites. This ratio was recommended based on a simulation-based model for estimating resonant-like amplification behaviour [40–42], which is consistent with the site amplification factors of around 2 (for high shaking level) to 3 (for low shaking level) estimated using the NGA-West models, as reported in Abrahamson et al. [43] and Huang et al. [44]. A uniform level of site amplification has been adopted in this study for simplicity.

The calculation shows that the case study building, as represented by the sub-structure model, has an annual rate of collapse of 4.6×10^{-5} if the numerical model was calibrated to the QS results, which corresponds to a 0.23% chance of collapse in 50 years and is lower than the 1% limit stipulated in IBC and ASCE/SEI 7. This is also lower than the proposed risk limit of 0.3% in 50 years for this type of RC structure in order to control the individual annual fatality risk in an ordinary building (i.e. Risk Category II in ASCE 7) to the tolerable level of 10^{-6} [45–47]. However, if the assessment is based on the numerical model that was calibrated to the HS results, the collapse rate would double, i.e. 9.2×10^{-5} or 0.46% in 50 years.

5. Conclusion

This paper aims to evaluate the effects of the application of conventional quasi-static (QS) versus hybrid simulation (HS) test results on collapse risk assessment outcomes. Two experiments were conducted on identical large-scale limited-ductile RC columns by the respective testing methods using the state-of-the-art Multi-Axis Substructure Testing (MAST) system, which is capable of controlling all six-degrees-of-freedom (6-DOF) boundary conditions in mixed load and deformation modes.

Larger flexural strength and a significant reduction in drift capacity resulted from the HS test due to the higher levels of axial loads. In addition, a lower level of cyclic degradations was observed in the HS test due to the ratcheting of the structure's lateral deformation, whereas the specimen experienced large cycles and load reversals before failure in the QS test. The hysteretic response behaviours from the QS and HS tests were then used respectively for calibrating the numerical models, which were employed for comparative collapse risk assessment.

The calculation shows that the structure has an annual rate of collapse of 4.6×10^{-5}, or 0.23% in 50 years, if the numerical model was calibrated to the QS results, whereas it is double, i.e. 9.2×10^{-5} or 0.46% in 50 years, if the numerical model was calibrated to the HS results. This shows the significance of the choice of experimental technique and the influence of axial load on the collapse risk assessment of structure.

6. Acknowledgments

The authors gratefully acknowledge the contribution of the Australian Research Council (Grants LE110100052, DP140103350, and DP1096753) and the Bushfire and Natural Hazards CRC. The authors would also like to acknowledge PhD student Scott Menegon for designing the structure.

7. References

[1] Vamvatsikos, D., and Cornell, C. A. [2002] Incremental dynamic analysis, *Earthquake Eng Struct Dyn*, vol. 31(3), pp. 491-514.

[2] Liel, A. B., and Deierlein, G. G. [2008] Assessing the collapse risk of california's existing reinforced concrete frame structures: Metrics for seismic safety decisions, The John A. Blume Earthquake Engineering Center, Stanford University, U.S.

[3] Celik, O. C., and Ellingwood, B. R. [2010] Seismic fragilities for non-ductile reinforced concrete frames - role of aleatoric and epistemic uncertainties, *Structural Safety*, vol. 32(1), pp. 1-12.

[4] Liel, A. B., Haselton, C. B., and Deierlein, G. G. [2011] Seismic collapse safety of reinforced concrete buildings. Ii: Comparative assessment of nonductile and ductile moment frames, *Journal of Structural Engineering (ASCE)*, vol. 137(4), pp. 492-502.

[5] Shoraka, M. B., Yang, T. Y., and Elwood, K. J. [2013] Seismic loss estimation of non-ductile reinforced concrete buildings, *Earthquake Engineering & Structural Dynamics*, vol. 42(2), pp. 297-310.

[6] Haselton, C. B., Liel, A. B., Lange, S. T., and Deierlein, G. G. [2008] Beam-column element model calibrated for predicting flexural response leading to global collapse of RC frame buildings, Pacific Earthquake Engineering Research Center, University of California Berkeley, U.S.

[7] Shoraka, M. B., and Elwood, K. J. [2013] Mechanical model for non ductile reinforced concrete columns, *Journal of Earthquake Engineering*, vol. 17(7), pp. 937-957.

[8] LeBorgne, M. R., and Ghannoum, W. M. [2014] Analytical element for simulating lateral-strength degradation in reinforced concrete columns and other frame members, *Journal of Structural Engineering (ASCE)*, vol. 140(7), p. 04014038.
[9] Ibarra, L. F., and Krawinkler, H. [2005] Global collapse of frame structures under seismic excitations, The John A. Blume Earthquake Engineering Center, Stanford University, U.S.
[10] Berry, M., Parrish, M., Eberhard, M. [2004] PEER structural performance database user's manual, Pacific Earthquake Engineering Research Center, University of California Berkeley, U.S.
[11] Sfakianakis, M. G., and Fardis, M. N. [1991] Bounding surface model for cyclic biaxial bending of RC sections, *Journal of Engineering Mechanics (ASCE)*, vol. 117(12), pp. 2748-2769.
[12] Bonet, J. L., Barros, M. H. F. M., and Romero, M. L. [2006] Comparative study of analytical and numerical algorithms for designing reinforced concrete sections under biaxial bending, *Computers & Structures*, vol. 84(31-32), pp. 2184-2193.
[13] Rodrigues, H., Furtado, A., and Arêde, A. [2015] Behavior of rectangular reinforced-concrete columns under biaxial cyclic loading and variable axial loads, *Journal of Structural Engineering*, DOI:10.1061/(ASCE)ST.1943-541X.0001345
[14] Lignos, D. G., Krawinkler, H., and Whittaker, A. S. [2011] Prediction and validation of sidesway collapse of two scale models of a 4-story steel moment frame, *Earthquake Eng Struct Dyn*, vol. 40(7), pp. 807-825.
[15] Suzuki, Y., and Lignos, D. [2014] Development of Loading Protocols for Experimental Testing of Steel Columns Subjected to Combined High Axial Load and Lateral Drift Demands Near Collapse, 10th US National Conference on Earthquake Engineering: Frontiers of Earthquake EngineeringAlaska, U.S.
[16] Krawinkler, H. [2009]. Loading histories for cyclic tests in support of performance assessment of structural components, 3rd International Conference on Advances in Experimental Structural Engineering, San Francisco, U.S.
[17] Dupuis, M. R., Best, T. D. D., Elwood, K. J., and Anderson, D. L. [2014] Seismic performance of shear wall buildings with gravity-induced lateral demands, *Canadian Journal of Civil Engineering*, vol. 41(4), pp. 323-332.
[18] Hashemi, M. J., and Mosqueda, G. [2014] Innovative substructuring technique for hybrid simulation of multistory buildings through collapse, *Earthquake Eng Struct Dyn*, vol. 43(14), pp. 2059-2074.
[19] Del Carpio Ramos, M., Mosqueda, G., and Hashemi, M. J. [2015] Large-scale hybrid simulation of a steel moment frame building structure through collapse, *Journal of Structural Engineering*, vol. 142(1), p. 04015086.
[20] Hashemi, M. J., Mosqueda, G., Lignos, D. G., Medina, R. A., and Miranda, E. [2016] Assessment of Numerical and Experimental Errors in Hybrid Simulation of Framed Structural Systems through Collapse, *Journal of Earthquake Engineering* (in press).
[21] Schellenberg, A. H., Mahin, S. A., and Fenves, G. L. [2009] Advanced implementation of hybrid simulation, Pacific Earthquake Engineering Research Center, University of California, Berkeley, U.S.
[22] French, C. E., Schultz, A. E., Hajjar, J. F., Shield, C. K., Ernie, D. W., Dexter, R. J., Du, D. H.-C., Olson, S. A., Daugherty, D. J., and Wan, C. P. [2004]. Multi-axial subassemblage testing (mast) system: Description and capabilities, 13th World Conference on Earthquake Engineering, Vancouver, Canada.
[23] Mahmoud, H. N., Elnashai, A. S., Spencer, B. F., Kwon, O. S., and Bennier, D. J. [2013] Hybrid simulation for earthquake response of semirigid partial-strength steel frames, *Journal of Structural Engineering (ASCE)*, vol. 139(7), pp. 1134-1148.
[24] Murray, J. A., and Sasani, M. [2016] Near-collapse response of existing RC building under severe pulse-type ground motion using hybrid simulation, *Earthquake Engineering & Structural Dynamics*, pp. n/a-n/a.
[25] Hashemi, M. J., Al-Mahaidi, R., Kalfat, R., and Burnett, G. [2015] Development and validation of multi-axis substructure testing system for full-scale experiments, *Australian Journal of Structural Engineering*, DOI:10.1080/13287982.2015.1092692
[26] Stojadinovic, B., Mosqueda, G., and Mahin, S. A. [2006] Event-driven control system for geographically distributed hybrid simulation, *Journal of Structural Engineering*, vol. 132(1), pp. 68-77.
[27] Federal Emergency Management Agency [2007] Interim testing protocols for determining the seismic performance characteristics of structural and nonstructural components, Department of Homeland Security (DHS), Washington D.C., U.S.
[28] Wibowo, A., Wilson, J. L., Lam, N. T. K., and Gad, E. F. [2014] Drift performance of lightly reinforced concrete columns, *Engineering Structures*, vol. 59pp. 522-535.
[29] Scott, M. H., and Fenves, G. L. [2006] Plastic hinge integration methods for force-based beam-column elements, *Journal of Structural Engineering*, vol. 132(2), pp. 244-252.
[30] Hashemi, M. J., Tsang, H.-H., Menegon, S., Rajeev, P., and Wilson, J. [2014] Modelling 3D Limited-Ductile RC Frame Structures for Collapse Risk Assessment, In: *Proceedings of the Australian Earthquake Engineering Society Conference*, Lorne, Australia

[31] Ibarra, L. F., Medina, R. A., and Krawinkler, H. [2005] Hysteretic models that incorporate strength and stiffness deterioration, *Earthquake Eng Struct Dyn*, vol. 34(12), pp. 1489-1511.

[32] Zhong, W. [2005] *Fast hybrid test system for substructure evaluation*, PhD Dissertation, University of Colorado Boulder, U.S.

[33] Schellenberg, A., Huang, Y., and Mahin, S. A. [2008]. Structural FE-Software Coupling through the Experimental Software Framework, OpenFresco, 14th World Conference on Earthquake Engineering, Beijing, China.

[34] PEER [2013] Structural performance database, Pacific Earthquake Engineering Research Center, University of California Berkeley, U.S.

[35] International Building Code (IBC) (2012). International Code Council, Country Club Hill, Illinois, U.S.

[36] ASCE/SEI 7-10, Minimum Design Loads for Buildings and Other Structures. (2010) Structural Engineering Institute (SEI), the American Society of Civil Engineers , Reston, Virginia, U.S.

[37] Somerville, P., Bayless, J., Skarlatoudis, A., Thio, H.K. (2013) Assessment of seismic design motions at low probabilities: comparing Australia and New Zealand. In: *Proceedings of the Australian Earthquake Engineering Conference*, Hobart, Tasmania, Australia, November 15-17, 2013.

[38] Tsang, H.H., Wilson, J.L., Lam. N.T.K. (2015). Recommended Site Classification Scheme and Design Spectrum Model for Regions of Lower Seismicity. In: *Proceedings of the Tenth Pacific Conference on Earthquake Engineering*, Sydney, Australia, November 6-8, 2015.

[39] Australian Standard: AS 1170.4-2007, Structural Design Actions, Part 4: Earthquake Actions in Australia. Standards Australia, Sydney, Australia.

[40] Tsang, H.H., Chandler, A.M., Lam, N.T.K. (2006). Estimating Non-linear Site Response by Single Period Approximation. *Earthquake Engineering and Structural Dynamics*, 35(9):1053-1076.

[41] Tsang, H.H., Chandler, A.M., Lam, N.T.K. (2006). Simple Models for Estimating Period-Shift and Damping in Soil. *Earthquake Engineering and Structural Dynamics*, 35(15):1925-1947.

[42] Tsang, H.H., Sheikh, M.N., Lam, N.T.K. (2012). Modeling Shear Rigidity of Stratified Bedrock in Site Response Analysis. *Soil Dynamics and Earthquake Engineering*, 34(1):89-98.

[43] Abrahamson, N., Atkinson, G., Boore, D., Bozorgnia, Y., Campbell, K., Chiou, B., Idriss, I.M., Silva, W., Youngs, R. (2008). Comparisons of the NGA ground-motion relations. *Earthquake Spectra*, 24(1): 45-66.

[44] Huang, Y.-N., Whittaker, A.S., Luco, N. (2010). NEHRP site amplification factors and the NGA relationships. *Earthquake Spectra*, 26(2): 583-593.

[45] ISO 2394:1998. General Principles on Reliability for Structures. International Organization for Standardization (ISO), Geneva.

[46] EN 1990: Eurocode: Basis of Structural Design (2002). European Committee for Standardisation (CEN), Brussels, Belgium.

[47] Tsang, H.H., Wenzel, F. (2016). Setting Structural Safety Requirement for Controlling Earthquake Mortality Risk. *Safety Science*, 86: 174-183.